RSC Advances

PAPER

View Article Online
View Journal | View Issue

Cite this: *RSC Adv.*, 2020, **10**, 17686

Mechanochemical approach to synthesize citric acid-soluble fertilizer of dittmarite ($NH_4MgPO_4 \cdot H_2O$) from talc/$NH_4H_2PO_4$ mixture†

Yonghao Tan, Lin Sha, Nengkui Yu, Zhengshuo Yang, Jun Qu * and Zhigao Xu*

In this study, a citric acid-soluble fertilizer of dittmarite ($NH_4MgPO_4 \cdot H_2O$) was synthesized by balling talc with $NH_4H_2PO_4$. The effects of ball milling speed and milling time on the dissolution rates of N, P and Mg in deionized water and 2% citric acid were explored. Characterization technologies such as X-ray diffraction (XRD), Fourier transform infrared spectroscopy (FT-IR), thermogravimetric analysis (TG) and Scanning electron microscopy (SEM) were applied to test the prepared samples. In water, the prepared dittmarite was changed into struvite ($NH_4MgPO_4 \cdot 6H_2O$) with almost no N, P or Mg release, while the dissolution rates of nutrient elements reached almost 100% in 2% citric acid. The proposed work presented a facile and environmentally friendly method to produce CASF with high agricultural and ecological value.

Received 14th January 2020
Accepted 30th April 2020

DOI: 10.1039/d0ra00387e

rsc.li/rsc-advances

1 Introduction

Slow-release fertilizer can release nutrients in the entire growth cycle of crops with the advantages of low fertilizer dosage and high nutrient utilization rate.[1–4] Citric acid-soluble fertilizer (CASF) is a type of slow-release fertilizer, the nutrients of which can be dissolved in acidic solution while remaining unchanged in neutral or alkaline environment.[5] The nutrients in CASF do not migrate with flowing water but can be dissolved (by organic acid secreted from the root system) and adsorbed by crops, acting as slow-release fertilizer.[6,7] The utilization of CASF can effectively avoid harmful migration of nutrients (groundwater pollution), especially in rainy areas, which is a common problem in regions with excessive use of water-soluble fertilizers.[8] Therefore, CASF can partially substitute widely used water-soluble fertilizers for the purpose of reducing agricultural production cost and environmental pollution.

The commonly used CASF is citric acid-soluble phosphate fertilizer, yet increasing published works has been putting efforts towards developing other types of CASF with various nutrients.[9] Magnesium ammonium phosphate (struvite $NH_4MgPO_4 \cdot 6H_2O$ and dittmarite $NH_4MgPO_4 \cdot H_2O$) can act as excellent CASF with high content of Mg, N and P elements. The natural mineral form of magnesium ammonium phosphate is struvite ($NH_4MgPO_4 \cdot 6H_2O$). However, the struvite deposit is relatively rare. The reserves are too small for large-scale applications for agricultural production.[10] The researchers have developed several methods for the synthesis of struvite based on the co-precipitation mechanism of Mg^{2+}, NH_4^+, and PO_4^{3-} in the solution.[11,12] The precipitation process was an effective way to eliminate NH_4^+ and PO_4^{3-} pollutants in the industrial wastewater[13–16] or agricultural sewage,[17] from which the struvite could be obtained. Although the mentioned work above could achieve the goal of water purification and resource recovery from nitrogen and phosphorus polluted water at the same time, the low yield limited its large-scale production. Moreover, using soluble salts as raw materials to produce struvite will lead to N and O residual in the solution. New green approaches to synthesize magnesium ammonium phosphate should be developed for its practical application in agriculture.

The high-energy ball milling process, also known as the mechanochemical approach, has been intensely reported in multiple areas.[18] However, most of the results were achieved from lab work which could not be industrialized due to the lack of industrial equipment. Recent years, the solvent-free mechanochemical process has gradually become a mature industrial craft especially in the area of powder metallurgy[19] and environmental pollutant degradation[20] with the continuous development of industrial-scale high energy ball mill equipment.[21,22] A horizontal planetary ball mill (continuous powder discharge system by negative pressure) was developed in China for the crushing and activation of cement raw materials with energy consumption abatement by 40% compared with the traditional ball milling equipment.[23] Environmental Decontamination Ltd. (EDL) company from New Zealand developed a system of dry horizontal stirred mill[24] and Radicalplanet® Research Institute Co. Ltd. produced an intermittent vertical planetary ball mill for

Key Laboratory of Catalysis and Energy Materials Chemistry of Ministry of Education, Hubei Key Laboratory of Catalysis and Materials Science, College of Resources and Environmental Science, South-Central University for Nationalities, Wuhan 430074, China. E-mail: qujun2018@scuec.edu.cn; xuzhigaotc@126.com

† Electronic supplementary information (ESI) available. See DOI: 10.1039/d0ra00387e

the remediation of organic contaminated soil.[25] The ball milling process has been proved to be an effective way for the production of CASF in the lab.[26–28] Borges *et al.*[29–33] conducted a series of work on the mechanochemical conversion of clay minerals (talc, chrysotile and montmorillonite) into slow-release fertilizer by mechanochemical approaches. Amorphous product or K-struvite phase was obtained after the ball milling operation. Magnesium ammonium phosphate salt of dittmarite (formula of $NH_4MgPO_4 \cdot H_2O$ with excellent CASF properties) has also been manufactured by milling $Mg(OH)_2$ with $NH_4H_2PO_4$.[34] Combing with the lab work, the industrial high energy ball milling equipment will promise the practical production of CASF by the mechanochemical approach.

Magnesium element has a great agricultural value such as quality improvement and yield increasing of crops.[35] Some studies have directly applied magnesium silicate mineral (serpentine) as fertilizer for crops.[36] Talc ($Mg_3Si_4O_{10}(OH)_2$) is a widely distributed magnesium-rich silicate mineral that is usually crushed into powder state for application in the paper industry, pharmaceutical industry, cosmetics industry and *etc.*[37] Only high-grade talc can be applied in the above industries while a tremendous amount of low-grade talc or talc-rich tailings from the mineral separation process was underutilized.[38] Developing new processes to transform talc into fertilizer will not only help to expand the application field of talc but also recycle the talc waste.

In this study, talc was milled with $NH_4H_2PO_4$ for the first time to directly produce dittmarite phase serving as citric acid-soluble fertilizer. The ground samples were respectively stirred in water and 2% citric acid and then the dissolution rates of Mg, N, and P elements were studied. The obtained data confirmed that after ball milling operation the water-soluble N and P from $NH_4H_2PO_4$ and water-insoluble Mg from talc were transformed into citric acid-soluble ones. Multiple methods such as XRD, FT-IR, TG-DSC and SEM have been applied to illustrate the mechanism of dittmarite formation and nutrient elements releasing. The proposed process was easy to operate with no wastewater generation or gas emission. The partial replacement of water-soluble fertilizer with the prepared CASF can help reduce the cost of agricultural production and the harmful effects of fertilizer on the environment.

2 Experimental procedure

2.1 Materials and methods

Block talc mineral was purchased from Guangzhou Huajun talc powder Co., Ltd which came from Guangdong province, China. Manual crushing by rubber hammer and mortar was applied to obtain talc powder (<100 mesh). Ammonium dihydrogen phosphate ($NH_4H_2PO_4$) and citric acid were of analyst grade and used without further treatment (Aladdin Co Ltd., Shanghai, China). Milli-Q ultrapure water (18.2 MΩ cm) was used in this work.

A planetary ball mill equipment (PM-100, Retsch, Germany) was applied for the synthesis of CASF. 0.5 g talc and 0.4563 g $NH_4H_2PO_4$ (according to the reaction in eqn (1)) were mixed and put into a steel ball mill jar (50 cm^3) which was filled with one 17 mm (diameter), four 15 mm (diameter) and twenty 5 mm (diameter) steel balls. During the ball milling process, the milling speed was varied between 0–600 rpm and the milling time was controlled between 0–60 min. The ground sample at 600 rpm for 60 min was labeled as D-600.

$$Mg_3Si_4O_{10}(OH)_2 + 3NH_4H_2PO_4 \rightarrow 3NH_4MgPO_4 \cdot H_2O + H_2SiO_3 \cdot 3SiO_2 \quad (1)$$

0.3 g of the ground sample was stirred in 30 ml 2% citric acid (simulating the acid environment around the root of crops according to ref. 6) and 30 ml deionized water respectively on an air thermostatic oscillator (THZ-C, Peiying Experimental equipment, Suzhou, China) for 2 h at 25 °C. Afterwards, the obtained suspensions were filtered by polyethersulfone membrane (PES 25 um, Jing Teng, Shanghai, China) to separate the solid and the solution. The residual solid was dried in a glass dryer with silica gel and collected for various characterizations. The solution was diluted to measure the concentration of Mg^{2+} (ICP-OES, Avio 200, PerkinElmer, America), NH_4^+ (Nessler's reagent spectrophotometry, Chinese National Environmental standard HJ 535-2009) and PO_4^{3-} (ammonium molybdate spectrophotometry, Chinese National standard GB/T 11893-1989). A UV-vis spectrophotometer (Lambda 365, PerkinElmer, America) was used for the concentration test of NH_4^+ and PO_4^{3-}.

2.2 Characterization techniques

The XRD patterns of the samples were tested on a Rigaku MAX-RBRU-200B diffractometer (Rigaku, Japan) at the 2-theta degree of 5°–70°. The microstructures of the obtained samples were characterized by an SEM spectroscopy (JSM-5610LV, JEOL, Japan). TG-DSC data were collected on a simultaneous thermal analyzer (STA449F3, NETZSCH, Germany) in N_2 atmosphere from room temperature to 1000 °C. FT-IR spectra of the samples were recorded on Nicolet 6700 (Thermo, American) using KBr as a diluent over 4000–500 cm^{-1}.

3 Results and discussion

The XRD patterns of raw talc and the ground sample (60 min milling time) with milling speed varied at 150 rpm, 300 rpm, 450 rpm, and 600 rpm are illustrated in Fig. 1. The raw material observed an integral XRD pattern of talc with weak peaks from impurities. The content of the Mg element in raw material was 18.5% (dissolved in HF and HNO_3 mixed solution and tested by ICP-OES) which was close to the theoretical Mg content of talc (19.05%), indicating a high grade of talc in the raw material. Milling talc with $NH_4H_2PO_4$ at a low speed of 150 rpm made no changes to the raw materials mixture.[39] The peak intensity of talc and $NH_4H_2PO_4$ gradually decreased with the increase of grinding speed. The diffraction peaks of $NH_4H_2PO_4$ disappeared and just (002) and (006) peaks of talc were left at milling speed of 450 rpm. Furthermore, the talc (002) peak position of 450 rpm sample shifted from 9.44 Å to 9.31 Å indicating that the balling process induced the changes and collapse of the layered structure of talc. Precursor phase of

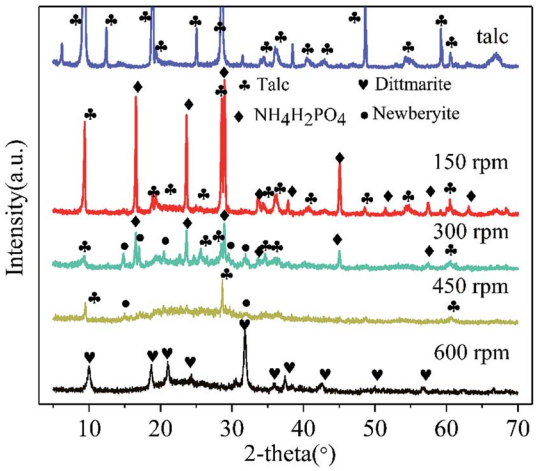

Fig. 1 XRD patterns of raw talc and samples milled at different speeds (60 min milling time).

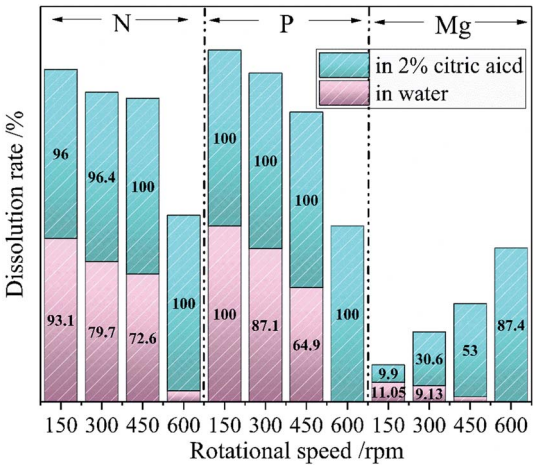

Fig. 2 The Mg, P, and N dissolution rates of the ground sample at different milling speed (60 min milling time) in water (pink) and 2% citric acid (green).

newberyite ($MgHPO_4 \cdot 3H_2O$ JCPDS 35-0780) was observed in 300 rpm sample. When the milling speed reached 600 rpm, a pure phase of dittmarite ($NH_4MgPO_4 \cdot H_2O$)[34] was formed without newberyite. The essential information of X-ray diffraction peaks of talc, $NH_4H_2PO_4$ (JCPDS 37-1479), and the ground samples at different speeds were listed in Table 1. The XRD data proved that talc would just react with the anionic part of $NH_4H_2PO_4$ (PO_4^{3-}) to form newberyite ($MgHPO_4 \cdot 3H_2O$) at low milling speed. High grinding speed of 600 rpm triggered the solid reaction between $NH_4H_2PO_4$ and talc forming the dittmarite phase.

The nutrients release experiments (in deionized water and 2% citric acid respectively) were conducted to evaluate the citric acid and water solubility of the ground samples. The Mg, P, and N dissolution rates of the samples ground at different milling speeds in water and 2% citric acid respectively with grinding time of 60 min are depicted in Fig. 2. The dissolution rates of the P and N decreased from 100% to nearly 0% with the increase of milling speed when stirring the ground sample in deionized water. That meant the water-soluble N and P from $NH_4H_2PO_4$ had been transformed into water-insoluble forms. A dissolution rate of 11.05% also dropped to nearly 0% for Mg elements which came from talc. Mechanochemical activation of the mineral would generally increase its solubility rather than decrease the solubility. Aglietti[40] explored the effect of dry grinding on the structure of talc. The increase of soluble Mg content of the prepared samples was observed after the high energy ball milling operation. Therefore, the decrease of Mg content in this work after ball milling could be related to phase transformation rather than mechanochemical activation. In 2% citric acid, the dissolution rates of P and N kept at 100% and Mg gradually increased from 9.9% to 87.4% as the speed of ball milling raising from 150 rpm to 600 rpm. The above data clarified that the milling operation converted the water-soluble N and P into water-insoluble but citric acid-soluble forms; the water-insoluble Mg from talc into citric acid-soluble forms. The changes in the dissolution rates of Mg, P and N could be related to the phase transformation of the raw mixture upon the increase of milling speed. After high energy ball milling of talc and $NH_4H_2PO_4$, the formed dittmarite showed the typical characteristic of CASF for Mg, P and N elements.

According to the above analysis, the optimal ball-milling speed was 600 rpm at which a complete reaction between the raw materials took place. Talc and $NH_4H_2PO_4$ mixture could be successfully converted into dittmarite serving as CASF. The following experiments explored the effect of ball grinding time on the dissolution rate of each element to further illustrate the solid phase transformation process. The Mg, P and N dissolution rates of the ground sample in deionized water and 2% citric

Table 1 The X-ray diffraction peaks of talc (JCPDS 29-1493), $NH_4H_2PO_4$, and the ground samples at different speeds

Sample	Main phase	Characteristic three strong peaks (relative intensity order)
Talc	Talc	9.44 Å (002), 3.13 Å (006) and 4.60 Å (−111)
$NH_4H_2PO_4$	$NH_4H_2PO_4$ (JCPDS 37-1479)	5.32 Å (101), 3.07 Å (211) and 3.75 Å (200)
150 rpm sample	$NH_4H_2PO_4$	9.4 Å (002), 3.12 Å (006) and 4.58 Å (−111)
	Talc	5.35 Å (101), 3.08 Å (211) and 3.76 Å (200)
300 rpm sample	$NH_4H_2PO_4$	9.46 Å (002), 3.13 Å (006) and 4.59 Å (−111)
	Talc	5.35 Å (101), 3.08 Å (211) and 3.76 Å (200)
	Newberyite	3.02 Å (113), 3.47 Å (221) and 5.98 Å (111)
450 rpm sample	Talc	9.31 Å (002) and 3.12 Å (006)
600 rpm sample	Dittmarite (JCPDS 36-1491)	8.77 Å (010), 2.8 Å (200) and 2.92 Å (030)

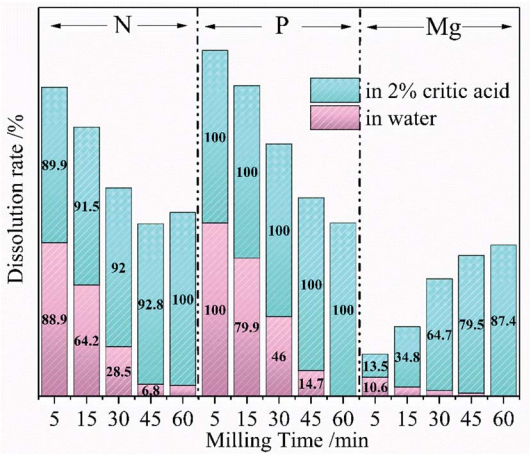

Fig. 3 The Mg, P, and N dissolution rates of the ground sample at different milling time (600 rpm milling speed) in water (pink) and 2% citric acid (green).

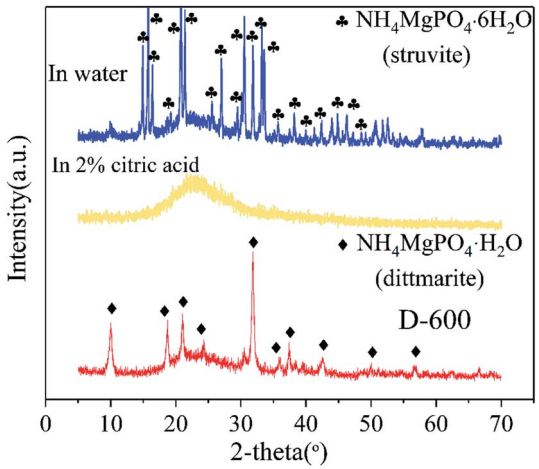

Fig. 4 XRD patterns of D-600 sample, D-600 sample after agitation in deionized water and D-600 sample after agitation in 2% citric acid.

acid at different milling time with the grinding speed of 600 rpm are exhibited in Fig. 3. The P element of the milled samples showed constant high dissolution rates (close to 100%) in citric acid solution, while the rates gradually decreased to 0% in deionized water with the increase of milling time. At the same time, the Mg dissolution rate decreased from 10.6% to 0% in deionized water and raised from 13.5% to 87.4% in citric acid. Theoretically, Both P and N in the sample should be 100% soluble in 2% citric acid. The content loss of N was observed in the N dissolution data of Fig. 2 (150 rpm and 300 rpm) and Fig. 3 (5–45 min). Aglietti[40] confirmed that ball milling operation would increase the Mg dissolution rate of talc in water accompanied with the increase of pH value (OH^- release). The XRD data in Fig. 1 proved that the low milling speed could not induce the formation of the dittmarite phase which was surely the same results with short milling time. Therefore, the anionic part of $NH_4H_2PO_4$ (PO_4^{3-}) was fixed by reacting with the Mg from the milled talc. A small part of NH_4^- would react with OH^- from the activated talc and released as ammonium gas which resulted in the N mass loss as shown in Fig. 2 (150 rpm and 300 rpm) and Fig. 3 (5–45 min). The difference in the release characteristics of elements in different solvents were closely related to the phase changes during the ball milling process. $NH_4H_2PO_4$ was very soluble in water and citric acid, while the nature mineral of talc (magnesium silicate and rich in hydroxyl group) was insoluble in water and slightly soluble in citric acid. At low milling speed, the release characteristics of N, P and Mg was highly depended on the soluble property of $NH_4H_2PO_4$ and talc. After high ball milling process, talc reacted with $NH_4H_2PO_4$. The nutrients of N, P and Mg formed the phase of dittmarite which was insoluble in water but very soluble in citric acid. The data in Fig. 3 was consistent with the data in Fig. 2 that meant a necessary milling time was needed for the reaction between talc and $NH_4H_2PO_4$ to form the phase of dittmarite.

XRD patterns of D-600 sample, D-600 sample after agitation in deionized water and D-600 sample after agitation in 2% citric acid are depicted in Fig. 4 to explain the mechanism of nutrients dissolution. The D-600 sample with a phase of dittmarite ($NH_4MgPO_4 \cdot H_2O$) was transformed into struvite after agitation in water. However, the D-600 sample after agitation in 2% citric acid observed no obvious crystalline phase forming an amorphous substance. The XRD data revealed that the ground sample held the nutrients by forming high crystalline struvite in deionized water. In 2% citric acid, the prepared dittmarite was completely dissolved to release the Mg, P and N elements. Struvite was the natural mineral form of magnesium ammonium phosphate salts and could stably exist in the natural environment to form a deposit. Solihin *et al.*[34] has also proved the stable property of struvite prepared by ball milling in water for 500 hours. However, transformation of dittmarite to struvite would be influenced by the practical soil conditions. Much work[11,41] has explored the optimal pH value for the crystallization of struvite in industrial wastewater or domestic sewage (a more complicated solution environment than that of in the soil). A neutral or alkaline environment was conducive to the

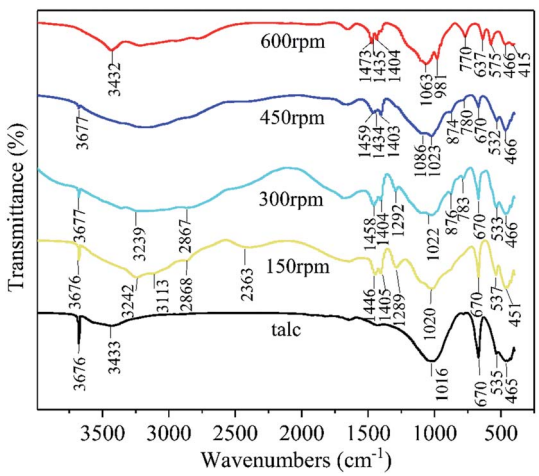

Fig. 5 FT-IR patterns of talc, the milled products at 150 rpm, 300 rpm 450 rpm and 600 rpm (60 min milling time).

crystallization of struvite. In this work, the obtained data also proved the stable property of struvite in a neutral environment and could be dissolved in acid solution. The prepared product would stably exist in neutral or alkaline soil, and be dissolved by the plant acid secreted from the root of crops as a long-acting CASF. In acidic soil, struvite would be directly dissolved and cannot act as CASF. Therefore, the dittmarite product in this work was suitable for application in neutral and alkaline soils.

The FT-IR analysis was used to illustrate the chemical bonding changes in the solid reaction process. The FT-IR patterns of talc and the milled samples (60 min milling time) at different milling speeds of 150 rpm, 300 rpm, 450 rpm, and 600 rpm are displayed in Fig. 5. The detailed infrared information of talc,[39] $NH_4H_2PO_4$,[42] and the ground samples at different speeds were listed in Table 2. The 150 rpm sample found both infrared bands from talc and $NH_4H_2PO_4$ which was consistent with the XRD data in Fig. 1 (a mixture of talc and $NH_4H_2PO_4$ was observed). Increasing the milling speed caused that the peaks of talc and $NH_4H_2PO_4$ gradually faded away, while the 600 rpm sample showed an entire new FT-IR pattern. The decrease of peak strength and disappearance of the peaks from talc indicated the destruction of talc crystalline structure which was triggered by the high energy ball milling. The infrared bonds of talc and $NH_4H_2PO_4$ were gradually replaced by newly formed chemical bonds. The FT-IR pattern of 600 rpm showed the characteristic infrared peaks of magnesium ammonium phosphate salt which consisted with the FT-IR data of struvite.[43] The Si–O stretching vibration at 1016 cm^{-1} from talc shifted to 1080 cm^{-1} which fitted to Si–O–Si asymmetric bond stretching vibration.[44] Combining with the XRD data in Fig. 1, in which the 600 rpm sample showed no crystalline phase of silicate, the frequency shift of S–O vibration could be attributed to the structure destruction of talc and formation of amorphous silica by the high energy ball milling.

The summarized results of TG/DSC of talc and the D-600 sample is displayed in Fig. 6. The thermal decomposition of talc occurred between 830 °C and 1000 °C to form clinoenstatite, and the mass loss rate was about 4.67%.[39] A totally different TG and DSC curves were obtained after milling talc with $NH_4H_2PO_4$ at 600 rpm. When the temperature reached 250 °C, the 22.73% mass loss could be attributed to the release of one crystal water and one ammonia molecule in $NH_4MgPO_4 \cdot H_2O$.[34,46] The DSC curve of D-600 sample has two sharp peaks at about 200 °C and 700 °C. The endothermic peak at about 200 °C was caused by the removal of one crystal water in $NH_4MgPO_4 \cdot H_2O$, and the exothermic peak at about 700 °C could be attributed to the decomposition of NH_4MgPO_4.[46] The TG-DSC curve of the grinding sample was similar to that of the struvite except for the mass loss of crystal water indicating the successful preparation of dittmarite.

The microstructure and elements distribution of the D-600 sample was tested on an SEM equipment (Fig. 7). Plate-like and flakey particles were observed in the SEM image of the D-600 sample. Mg, N, and P elements possessed similar

Table 2 The infrared absorption peaks of talc,[39] $NH_4H_2PO_4$,[42] and the ground samples at different speeds (60 min milling time)

Sample	Frequency (cm^{-1})	Assignment
Talc	3676	OH stretching vibration
	670	OH rocking vibration
	1016	Si–O stretching vibration
	535 and 465	Coupling vibration of Si–O bending vibration and M–O vibration
$NH_4H_2PO_4$	3240 and 3100	NH_4^+ vibration
	2860	N–H vibration
	2387	Band of hydrogen bond
	1448 and 1398	Bending vibration of ammonium
	1300	$H_2PO_4^-$ vibration
150 rpm sample	3676 and 670; 1020; 537 and 451	Vibration from talc: OH vibration; Si–O stretching vibration; Si–O and M–O vibration
	3242 and 3113; 2868; 2363; 1446 and 1405; 1289	Vibration from $NH_4H_2PO_4$: NH_4^+ vibration; N–H vibration; hydrogen bond vibration; ammonium vibration; $H_2PO_4^-$ vibration
300 rpm sample	3677 and 670; 1022; 533 and 466	Vibration from talc: OH vibration; Si–O stretching vibration; Si–O and M–O vibration
	3239; 2867; 1458 and 1404; 1292	Vibration from $NH_4H_2PO_4$: NH_4^+ vibration; N–H vibration; ammonium vibration; $H_2PO_4^-$ vibration
	876; 783	**New peaks: P–O–H vibration;[42] water–water H bonding[45]**
450 rpm sample	3677 and 670; 1023; 532 and 466	Vibration from talc: OH vibration; Si–O stretching vibration; Si–O and M–O vibration
	1459 and 1403	Vibration from $NH_4H_2PO_4$: ammonium vibration
	1434; 1086; 874; 780	**New peaks: split of NH_4^+ bending vibration;[45] Si–O–Si asymmetric bond stretching vibration;[44] P–O–H vibration;[45] water–water H bonding[45]**
600 rpm sample	3432; 1473 and 1435; 1404; 981 and 1063; 770; 575	Vibration from dittmarite: NH_4^+ asymmetric stretching vibration; NH_4^+ split asymmetric bending vibration; ammonium vibration; antisymmetric stretching vibrations of PO_4^{3-}; water–water H bonding; P–O bend vibration of PO_4^{3-}
	1080; 466	Vibration from silicate: Si–O–Si asymmetric bond stretching vibration;[44] Si–O vibration

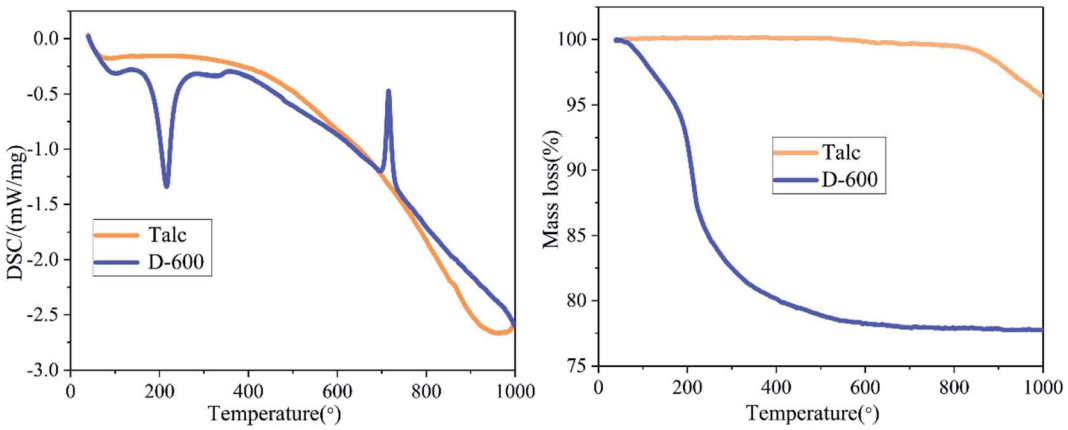

Fig. 6 TG (right) and DSC (left) patterns of talc and the D-600 sample.

distribution characteristics in the tested area which aggregated together to form major large particles in the field of view. Combing with the XRD data in Fig. 1, the large particles in the tested area could be attributed to the phase of dittmarite. Unlike Mg, N, and P elements, the Si element distributed evenly in the tested area which meant no crystalline silicate particles were formed. The orderly Si–O structure of talc was destroyed into disordered ones and dispersed in the product. The microstructure of raw talc and the D-600 sample was shown in the ESI (Fig. S-1).† The typical layered structure of talc was observed in the raw material. After ball milling with $NH_4H_2PO_4$, the layered structure was destroyed and agglomerated particles were formed in the submicron scale.

The above data clearly confirmed the successful synthesis of dittmarite by ball milling talc with $NH_4H_2PO_4$, which held the Mg, P, and N nutrients by the formation of struvite in water. In 2% citric acid, the prepared sample was dissolved to release nearly 100% nutrient elements. The difference in the release characteristics of elements in different solvents relayed on the phase changes during the ball milling process. At low milling speed, the release characteristics of N, P and Mg was highly depended on the soluble property of $NH_4H_2PO_4$ and talc. After high ball milling process, talc reacted with $NH_4H_2PO_4$. The nutrients of N, P and Mg formed the phase of dittmarite which was insoluble in water but very soluble in citric acid. The ground sample with typical characteristics of CASF could be used as a slow-release fertilizer. This facile and environmentally friendly process possessed great potential for the practical application, realizing the purpose of comprehensive utilization of talc-containing tailings and reducing the cost of agricultural production.

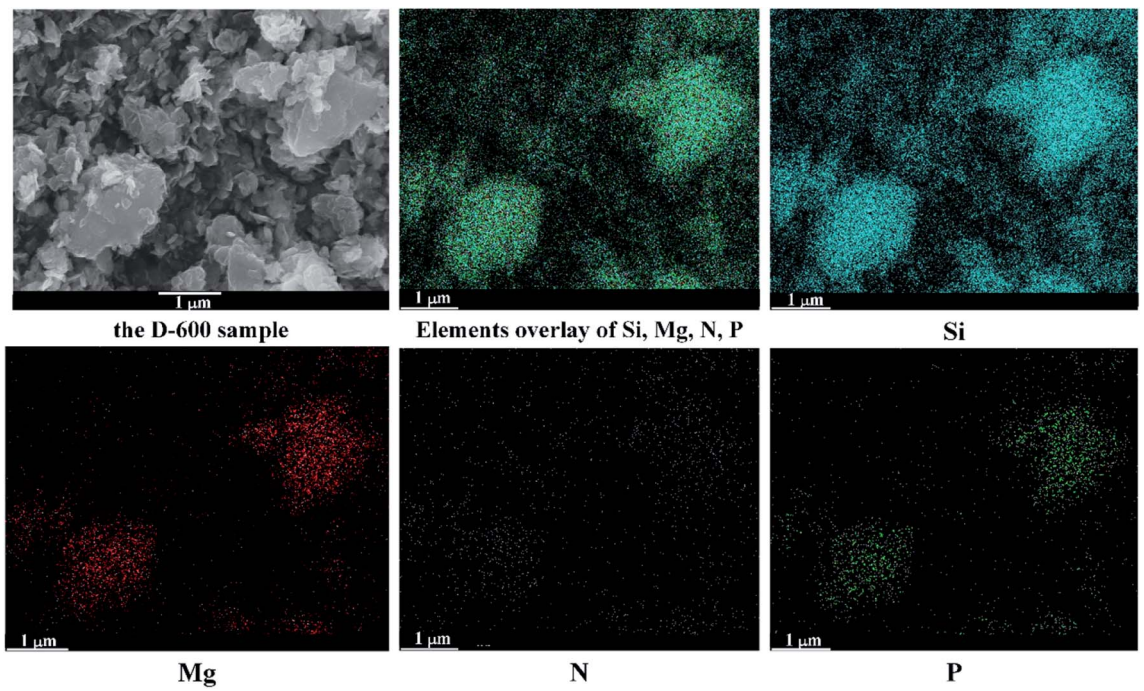

Fig. 7 The SEM image and element mapping of the D-600 sample.

4 Conclusion

A mechanochemical method was introduced to produce dittmarite to serve as a citric acid-soluble fertilizer by grinding talc with $NH_4H_2PO_4$. The ground sample held the Mg, N, and P with dissolution rates of nearly 0% by the mechanism of struvite formation in water. Nearly 100% of the nutrients elements in the prepared dittmarite could be dissolved in 2% citric acid which was the typical characteristic of CASF. The proposed craft was facile and environment-friendly with great potential for practical production. Partially replacing water-soluble fertilizers with the products in this study can effectively reduce agricultural production costs, control the harmful migration of nutrient elements, and achieve the goal of sustainable development of the agricultural system.

Conflicts of interest

There are no conflicts to declare.

Acknowledgements

This work is supported by the National Natural Science Foundation of China (No. 51904358 and 51734001), Natural Science Foundation of Hubei Province (No. 2019CFB267) and "the Fundamental Research Funds for the Central Universities", South-Central University for Nationalities (No. CZP19002, No. YZZ16002, and No. CZD 20007).

References

1 S. Chen, *et al.*, *Sci. Total Environ.*, 2018, **615**, 431–437, DOI: 10.1016/j.scitotenv.2017.09.209.
2 K. Min, *et al.*, *Environ. Sci. Pollut. Res.*, 2019, **2**, 1–13, DOI: 10.1007/s11356-019-05522-2.
3 K. Wu, *et al.*, *RSC Adv.*, 2019, **9**(55), 32270–32277, DOI: 10.1039/C9RA06939A.
4 Y. Zhang, *et al.*, *RSC Adv.*, 2018, **8**, 18146–18152, DOI: 10.1039/C8RA01843J.
5 S. C. Theophilus, *et al.*, *Environ. Sci. Pollut. Res. Int.*, 2017, **25**(20), 19298–19312, DOI: 10.1007/s11356-017-0385-4.
6 T. Imai, in *Phosphorus Recovery and Recycling*, ed. H. Ohtake and S. Tsuneda, Springer, Singapore, 1st edn, 2019, ch. 11, pp. 179–187.
7 Y. Chu, *et al.*, *Chem. Phys. Lett.*, 2020, **747**, 137347, DOI: 10.1016/j.cplett.2020.137347.
8 A. J. Camargo and A. Alonso, *Environ. Int.*, 2006, **32**, 831–849, DOI: 10.1016/j.envint.2006.05.002.
9 A. Said, *et al.*, *Appl. Clay Sci.*, 2018, **165**, 77–81, DOI: 10.1016/j.clay.2018.08.006.
10 S. Graeser, *et al.*, *Eur. J. Mineral.*, 2008, **20**(4), 629–633, DOI: 10.1127/0935-1221/2008/0020-1810.
11 K. S. Le Corre, *et al.*, *Environ. Sci. Technol.*, 2009, **39**(6), 433–477, DOI: 10.1080/10643380701640573.
12 K. Suzuki, *et al.*, *Bioresour. Technol.*, 2007, **98**(8), 1573–1578, DOI: 10.1016/j.biortech.2006.06.008.
13 L. Cubbage, *et al.*, *Proceedings of the Water Environment Federation*, 2011, (15), 228–238, DOI: 10.2175/193864711802862770.
14 D. Fang, *et al.*, *RSC Adv.*, 2018, **8**, 38013–38021, DOI: 10.1039/C8RA07876A.
15 X. Wang, *et al.*, *ACS Sustainable Chem. Eng.*, 2016, **4**(4), 2068–2079, DOI: 10.1021/acssuschemeng.5b01494.
16 K. Yetilmezsoy and Z. Sapci-Zengin, *J. Hazard. Mater.*, 2009, **166**(1), 260–269, DOI: 10.1016/j.jhazmat.2008.11.025.
17 E. Y. Lee, *et al.*, *Asian-Australas. J. Anim. Sci.*, 2015, **28**(7), 1053–1060, DOI: 10.5713/ajas.14.0679.
18 S. L. James, *et al.*, *Chem. Soc. Rev.*, 2012, **41**(1), 413–447, DOI: 10.1039/C1CS15171A.
19 Y. Lu, *et al.*, *Ceram. Int.*, 2013, **39**(4), 4421–4426, DOI: 10.1016/j.ceramint.2012.11.033.
20 G. Cagnetta, *et al.*, *J. Hazard. Mater.*, 2016, **313**, 85–102, DOI: 10.1016/j.jhazmat.2016.03.076.
21 Q. Zhang, J. Kano and F. Saito, *Powder Technol.*, 2007, **12**(7), 509–528, DOI: 10.1016/S0167-3785(07)12014-5.
22 J. Qu, *et al.*, *Appl. Clay Sci.*, 2016, **119**, 185–192, DOI: 10.1016/j.clay.2015.10.018.
23 X. Ye, *Mining & Processing Equipment*, 2015, **43**(12), 5–9, DOI: 10.16816/j.cnki.ksjx.2015.12.002.
24 D. J. Ducker, *Environ. Manag. Sustain. Dev.*, 2012, **1**(2), 163, DOI: 10.5296/emsd.v1i2.2170.
25 G. Cagnetta, J. Huang and G. Yu, *Crit. Rev. Environ. Sci. Technol.*, 2018, **48**(7–9), 723–771, DOI: 10.1080/10643389.2018.1493336.
26 M. Chen, *et al.*, *Process Saf. Environ. Prot.*, 2017, **114**, 91–96, DOI: 10.1016/j.psep.2017.12.008.
27 Solihin, *et al.*, *Powder Technol.*, 2011, **212**(2), 354–358, DOI: 10.1016/j.powtec.2011.06.012.
28 W. Yuan, *et al.*, *Powder Technol.*, 2014, **260**(7), 22–26, DOI: 10.1016/j.powtec.2014.03.072.
29 R. Borges, *et al.*, *Clay Miner.*, 2015, **50**, 153–162, DOI: 10.1180/claymin.2015.050.2.01.
30 R. Borges, *et al.*, *Clay Miner.*, 2016, **51**, 69–80, DOI: 10.1180/claymin.2016.051.1.06.
31 R. Borges, *et al.*, *Ind. Eng. Chem. Res.*, 2017, **56**, 708–716, DOI: 10.1021/acs.iecr.6b04378.
32 R. Borges, *et al.*, *J. Environ. Manage.*, 2018, **206**, 962–970, DOI: 10.1016/j.jenvman.2017.11.082.
33 R. Borges and F. Wypych, *J. Braz. Chem. Soc.*, 2019, **30**(2), 326–332, DOI: 10.21577/0103-5053.20180181.
34 Solihin, *et al.*, *Ind. Eng. Chem. Res.*, 2010, **49**, 2213–2216, DOI: 10.1021/ie901780v.
35 P. C. Smithson, *et al.*, *Nutr. Cycling Agroecosyst.*, 2004, **69**(1), 43–49, DOI: 10.1023/B:FRES.0000025294.96933.78.
36 E. T. Chittenden, *et al.*, *N. Z. J. Agric. Res.*, 1967, **10**(1), 160–171, DOI: 10.1080/00288233.1967.10423088.
37 A. Kalendova, D. Veselý and P. Kalenda, *Appl. Clay Sci.*, 2010, **48**(4), 581–588, DOI: 10.1016/j.clay.2010.03.007.
38 S. Farrokhpay, B. Ndlovu and D. J. Bradshaw, *Appl. Clay Sci.*, 2018, **160**, 270–275, DOI: 10.1016/j.clay.2018.02.011.
39 X. Liu, X. Liu and Y. Hu, *Clays Clay Miner.*, 2014, **62**(2), 137–144, DOI: 10.1346/CCMN.2014.0620206.

40 E. F. Aglietti, *Appl. Clay Sci.*, 1996, **9**, 139–147, DOI: 10.1016/0169-1317(94)90033-7.
41 M. M. Rahman, *et al.*, *Arabian J. Chem.*, 2014, **7**(1), 139–155, DOI: 10.1016/j.arabjc.2013.10.007.
42 C. Sun and D. Xue, *J. Phys. Chem. C*, 2013, **117**, 19146–19153, DOI: 10.1021/jp407947s.
43 R. L. Frost, M. L. Weier and K. L. Erickson, *J. Therm. Anal. Calorim.*, 2004, **76**, 1025–1033, DOI: 10.1023/b:jtan.0000032287.08535.b3.
44 A. Bertoluzza, *et al.*, *J. Non-Cryst. Solids*, 1982, **48**, 117–128, DOI: 10.1016/0022-3093(82)90250-2.
45 E. Banks, R. Chianelli and R. Korenstein, *Inorg. Chem.*, 1975, **14**(7), 1634–1639, DOI: 10.1021/ic50149a041.
46 A. A. Rouff, *J. Therm. Anal. Calorim.*, 2012, **110**(3), 1217–1223, DOI: 10.1007/s10973-011-2101-9.